Geology and geochemistry of giant quartz veins from the Bundelkhand Craton, central India and their implications

J K Pati[1,*], S C Patel[2], K L Pruseth[3], V P Malviya[1], M Arima[4], S Raju[5], P Pati[1] and K Prakash[1]

[1]*Department of Earth and Planetary Sciences, Nehru Science Centre, University of Allahabad, Allahabad 211 002, India.*
[2]*Department of Earth Sciences, Indian Institute of Technology, Powai, Mumbai 400 067, India.*
[3]*Department of Earth Sciences, Pondicherry University, Pondicherry 605 014, India.*
[4]*Graduate School of Environmental and Information Sciences, Yokohama National University, Tokiwadai, Hodogaya-ku, Yokohama 240 8501, Japan.*
[5]*Geological Survey of India (SR), Chennai 605 014, India.*
[*]*e-mail: jkpati@yahoo.co.in*

Giant quartz veins (GQVs; earlier referred to as 'quartz reefs') occurring in the Archean Bundelkhand Craton ($29,000\,km^2$) represent a gigantic Precambrian (~ 2.15 Ga) silica-rich fluid activity in the central Indian shield. These veins form a striking curvilinear feature with positive relief having a preferred orientation NE–SW to NNE–SSW in the Bundelkhand Craton. Their outcrop widths vary from ≤ 1 to 70 m and pervasively extend over tens of kilometers along the strike over the entire craton. Numerous younger thin quartz veins with somewhat similar orientation cut across the giant quartz veins. They show imprints of strong brittle to ductile–brittle deformation, and in places are associated with base metal and gold incidences, and pyrophyllite-diaspore mineralization. The geochemistry of giant quartz veins were studied. Apart from presenting new data on the geology and geochemistry of these veins, an attempt has been made to resolve the long standing debate on their origin, in favour of an emplacement due to tectonically controlled polyphase hydrothermal fluid activity.

1. Introduction

The giant quartz veins in the Bundelkhand Craton, central Indian shield constitute spectacular landforms in a regional scale (figure 1 modified after Basu 1986) because of their resistance to erosion, unique spatial disposition and homogeneous distribution with a preferred orientation spread over nearly $29,000\,km^2$. There are more than 1500 mappable quartz veins, presently exposed in the Bundelkhand Craton. Such veins are found in different parts of the world in similar settings (Kerrich and Feng 1992). The present study, apart from presenting salient field and petrographic observations, is the first attempt to discuss the significance of geochemistry of the quartz veins from the Bundelkhand Craton. It is also observed that K-feldspar which occurs as an accessory phase in minor to significant amounts in the bulk samples used in the present study has a dominant control on the geochemical trend of the GQVs.

2. Geology of the Bundelkhand Craton

The central Indian shield comprises the Aravalli, the Bundelkhand, and the Singhbhum cratons of Archaean–Proterozoic age. The Bundelkhand Craton is bound on its east, west and south by the Vindhyan Supergroup of rocks (figure 1). Its

Keywords. Quartz vein; Bundelkhand Craton; hydrothermal; central India.

J. Earth Syst. Sci. **116**, No. 6, December 2007, pp. 497–510

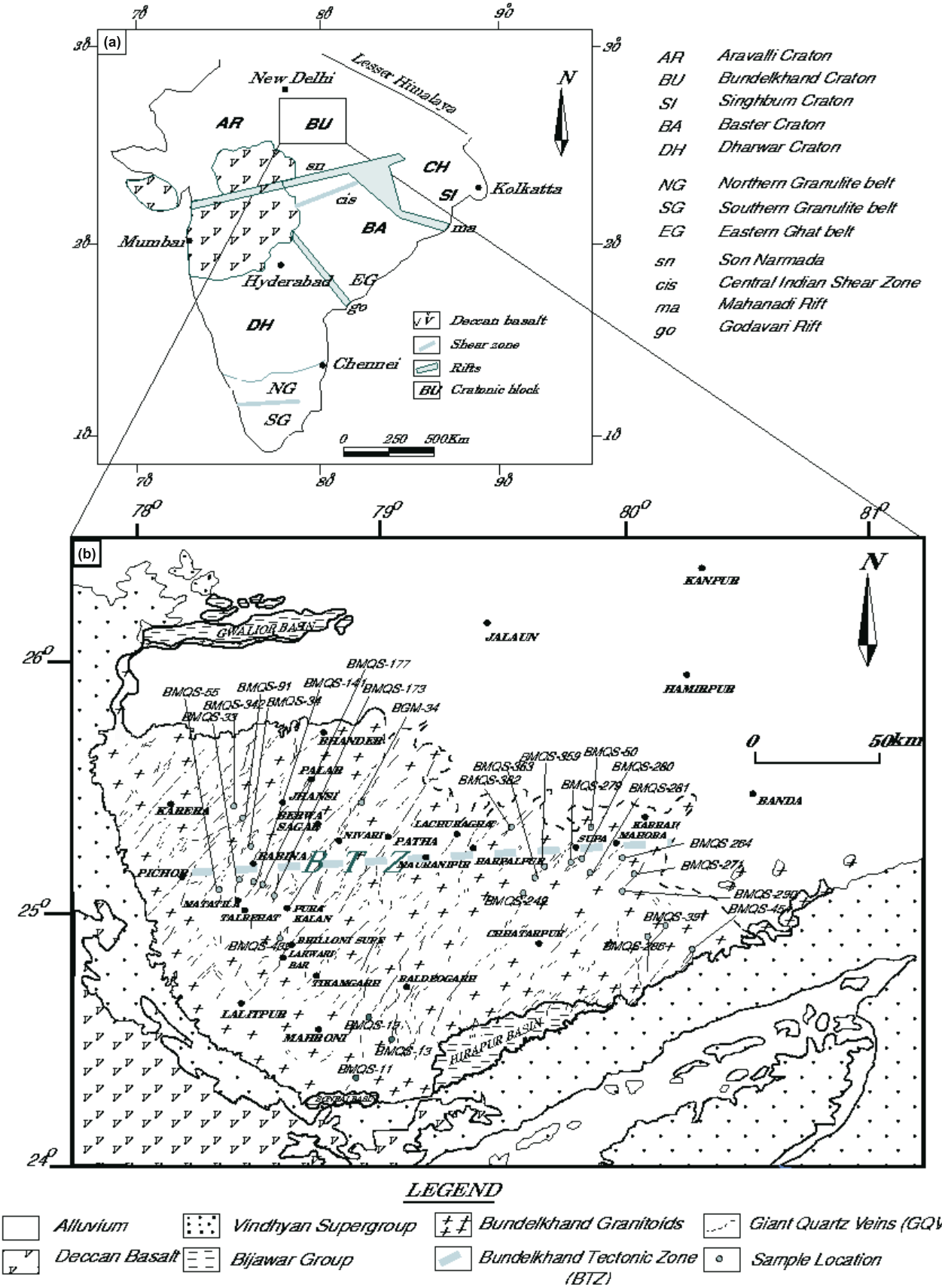

Figure 1. Location map showing Bundelkhand Craton in a generalized geological map of India (figure 1a), and the spatial distribution of giant quartz veins modified after Basu (1986) (figure 1b). NW-trending younger mafic dykes have not been shown for the sake of clarity. Thick dashed line in figure 1(b) marks the Bundelkhand Tectonic Zone, which is a crustal scale brittle–ductile shear zone.

south-western fringe is marked by a relatively small outcrop of the Deccan basalt and the northern part is hidden under the Indo-Gangetic alluvium. The Bundelkhand Granitoid Complex (BUGC) mainly comprises metamorphosed supracrustals (BIF, quartzites, gneisses, marbles, calc-silicates, amphibolites, and according to the recent findings by Malviya *et al* 2004 and 2006, pillow lavas, basaltic komatiites of boninitic affinity and volcaniclastic metasediments), plutonics (granitoids and rare syenites), and volcanics (rhyolites). The TTG (Tonalite-Trondhjemite-Granodiorite) gneisses, reported from the BUGC, record the oldest dates (3.3 Ga; Mondal *et al* 2002). The giant quartz veins were probably emplaced due to ongoing crustal movements subsequent to the stabilization of the cratonic segment at about 2.5 Ga. While the giant quartz veins, which are possibly of hydrothermal origin (2.0–1.9 Ga; Pati *et al* 1997) occupied the NE fracture swarms, the dolerite dykes which are of tholeiitic affinity (2.0–2.2 Ga; Rao *et al* 2005) settled in the NW trending fractures. The age of emplacement of the giant quartz vein is still uncertain. The K-Ar systematics followed in dating the micas may be related to post-emplacement shearing events. However, the cross cutting relationship with the mafic dyke suggests an age older than 2.0 Ga for the GQVs.

Studies on the structure and tectonics of the BUGC are rare, and are reported only for a few selected domains (Sharma 1982; Roday *et al* 1995; Prasad *et al* 1999). In all, five phases of deformation have been identified in the Bundelkhand Craton (Sharma 1982; Prasad *et al* 1999). For the first time, Senthiappan (1976, 1981) showed the presence of a nearly EW trending crustal-scale shear zone (Raksa Shear Zone) within the Bundelkhand Craton. The presence of a nearly EW trending crustal-scale brittle-ductile shear zone (Bundelkhand Tectonic Zone) extending across the Bundelkhand Craton at about 25°15′ N latitude has been revealed by recent field and remote sensing data (Pati 1998, 1999). Mineralizations in the BUGC include pyrophyllite-diaspore deposits associated with the giant quartz veins (Sharma 1979), incidences of shear zone-hosted gold (Pati *et al* 1997) and molybdenite (Pati 1999), and some other base metals in traces.

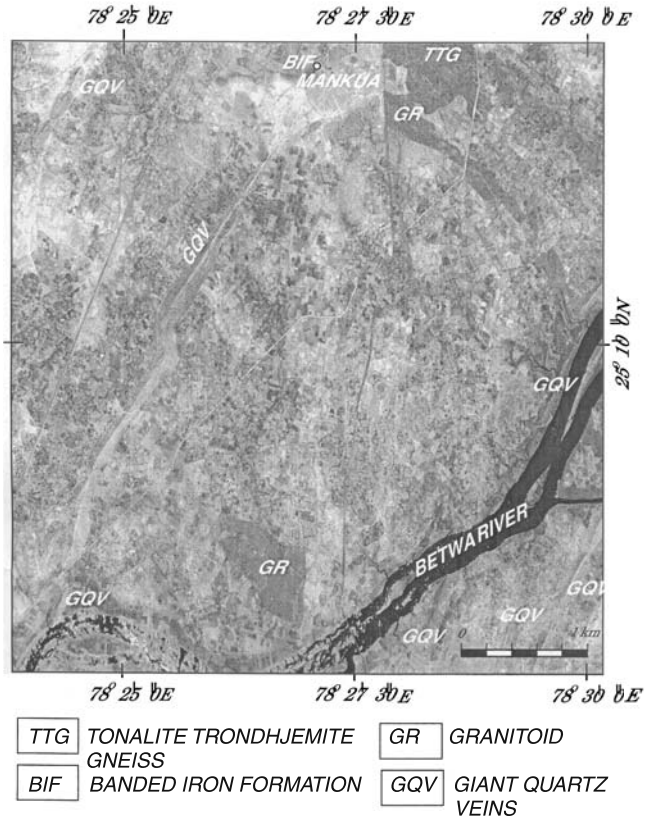

Figure 2. Indian Remote Sensing (IRS-1D) satellite image of parts of Mankua area, Jhansi district, Uttar Pradesh, showing sigmoidal and lenticular outcrop patterns of giant quartz veins (GQV) suggesting tectonic control of emplacement. An EW trending BIF band SW of Mankua village is truncated by a GQV.

3. Geology of giant quartz veins

The GQVs occur as cuesta-like features cropping out over the surrounding plain and are easily identified in topographic maps and LANDSAT TM and IRS (Indian Remote Sensing) satellite imageries due to their lighter tone and long linear-to-curvilinear disposition. Vegetation on their flanks gives the veins a darker tone and provides further contrast. The outcrop pattern of giant quartz veins is variable, but most veins are linear with very high aspect ratio and local sigmoidal geometry (figure 2). Such geometry suggests that the veins are emplaced along regional fault planes. Some of the veins occur as lenticular bodies, and at places, anastomosing types are also found. Large granitoid fragments (up to 1 m) are sometimes contained within the veins (figure 3b). Excellent breccia texture in the mesoscopic scale is also observed (figure 3d) suggesting that the veins underwent brittle deformation.

The maximum outcrop length of the giant quartz veins is more than 60 km (Basu 1986). However, they can be traced along the strike for over 100 km as discontinuous pinch and swell type outcrops with the average length of individual outcrops exceeding 1 km. Their width ranges from <1 m to $\sim$70 m with very few exceeding 20 m on the profile section. Debris on either sides of the giant quartz veins tend to increase the apparent width up to as large as 300 m noticed at Bar, Lalitpur district. In general, the GQVs are thicker at the middle and taper on both ends along their length.

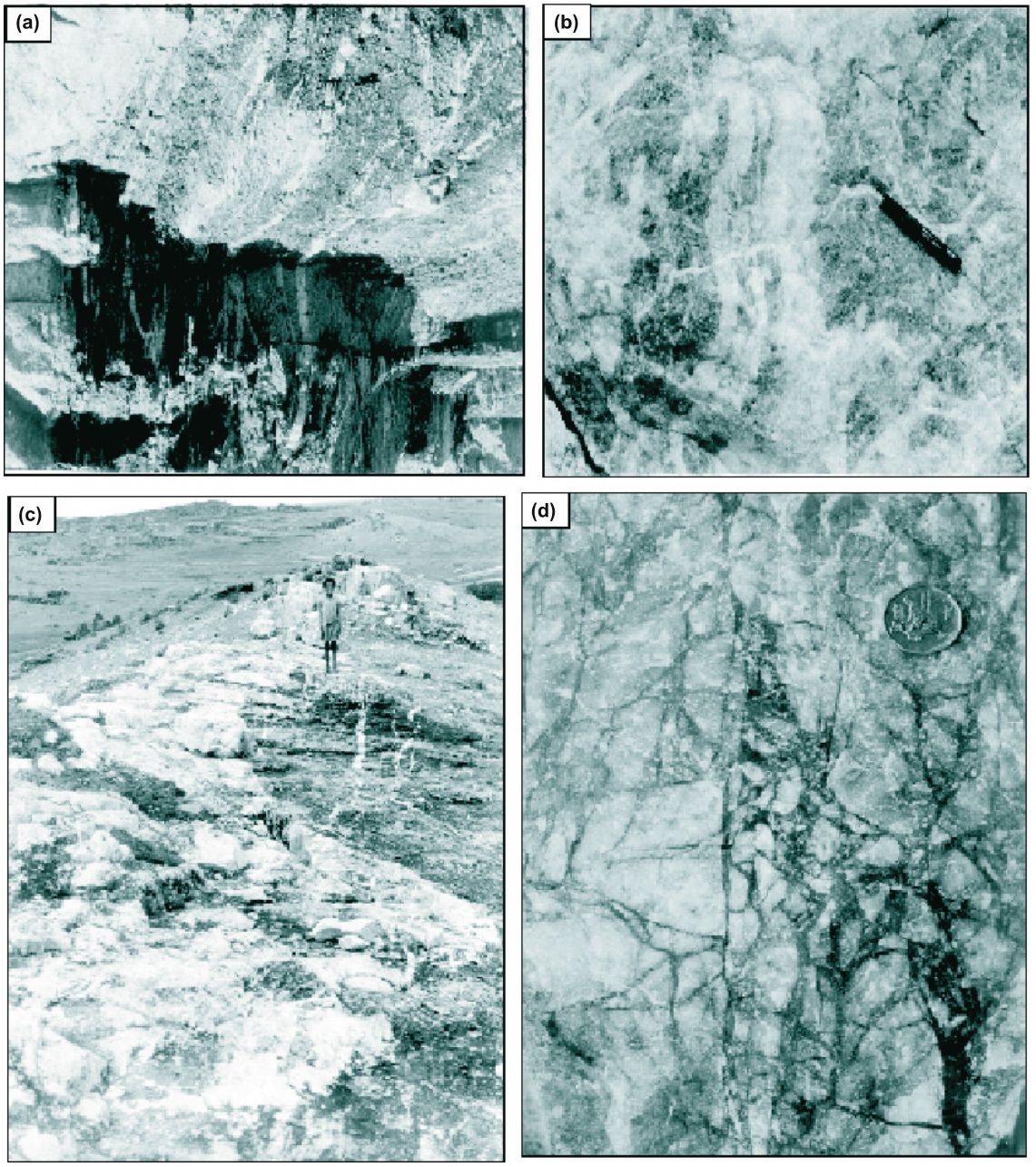

Figure 3. Field photographs. **(a)** Late generation thin quartz veins cut across the main vein suggesting multiple silica-rich solution activity in time and space in parts of Bundelkhand Craton. **(b)** Large granitoid clasts within giant quartz vein. Late generation thin quartz veins cut across the giant quartz vein as well as the granitoid clasts. **(c)** Giant quartz vein intruding the host coarse-grained pink granitoid ($\sim$2.5 Ga) with wavy contact. Some thin offshoot veins of quartz are present. **(d)** Breccia texture in giant quartz vein resulting from brittle deformation. Angular fragments of quartz are set in a fine-grained siliceous matrix.

The GQVs, in general, trend NNE–SSW with sub-vertical dips (figures 1, 2). Lateral veering of these veins is quite common and a few of them exhibit an EW orientation, some even showing NS to NNW–SSE trends. The prominent ones occur between Birdha and Bhuchera, to the NW of Bansi and north of Jamalpur, east of Rampur, and SE of Kotra (Lalitpur district). The EW trending GQVs occurring to the east of Bhainsai in the Mahoba district is an exception. In places, some of the veins are found to coalesce with or intersect each other, e.g., Jiraun Kasba of Jhansi district, Kandhari Kalan, Khariadhana, Bar and Patori of Lalitpur district and around Garhmau of Jhansi district. Interestingly, pyrophyllite-diaspore (Palar-Garhmau, Jhansi district; Larwari-Bar, Lalitpur district) and sporadic Cu mineralization (Karesara Kalan, Lalitpur district) are largely

confined to intersecting GQVs. Using this criterion, a few pyrophyllite-diaspore occurrences north and NNE of Pawagiri Jain Temple, Lalitpur district have been located (Pati, unpublished data).

The GQVs show wide variation in colour which is intriguing. There are four main types of GQVs based on colour, namely, milky white, shades of grey, hues of green, and shades of pink. The veins with local sigmoidal geometry are composed of green-coloured quartz and have comparatively higher associations with sulfides. The green colour is sometimes due to the presence of secondary epidote and chlorite. Very fine-grained green quartz similar to colloidal quartz is also observed in places. Quartz grains occurring within grey-coloured giant veins are highly strained in nature.

A number of thin (up to 10 cm; figure 3c) subvertical, milky white quartz veins occur largely subparallel to the GQVs and locally cut across them (figure 3a). In a number of places, thin offshoot veins of quartz are found to intrude the host granitoid (figure 3c). Purple-coloured amethyst is noted in quartz druses occurring within granitoids near Hasar Khurd and Barora, Lalitpur district. Colour in amethyst develops due to substitution of Fe^{3+} for Si followed by natural irradiation producing Fe^{4+} (Gaines *et al* 1997). It is possible that the presence of transition elements, impurities, lattice defects and strain have contributed to the variation of colour in the vein quartz. Gaines *et al* (1997) have noted that variable amounts of Al present in quartz may contribute to its colour.

Since Pascoe (1950) noted the GQVs to occur as ridges similar to walls within host granitoids, various workers have suggested contrasting models to account for their origin, but a definitive model is still lacking. On the basis of the "cataclastic and granulated nature and schistose structure" of these veins, Jhingran (1958) suggested that the veins are long narrow zones of intense mylonitization. However, on account of the opposite trends of GQVs with respect to the basic intrusives, he felt the situation to be intriguing and difficult to elucidate. Saxena (1961) considered these veins as superficial features and older than the granitoids. Mishra (1960) suggested that the GQVs are the result of recrystallization of earlier quartzites. Mishra and Sharma (1975) assigned a sedimentary origin to these veins based on evidences such as the presence of "cross beddings" and the occurrence of various "heavy minerals (such as authigenic zircon, glauconite, tourmaline and mica) within and along the primary surfaces". Basu (1986) suggested that these veins are of secreted silica emplaced along shears that are basically mylonites and further added that "mylonite formation" pre-dated the emplacement of GQVs. Sarkar *et al* (1994) pointed out that these are "intrusive quartz veins" possibly implying a magmatic origin.

4. Microscopic study

Randomly oriented sections of GQVs reveal that the samples are largely (>90 volume %) composed of quartz with minor-to-significant amounts of K-feldspar ± sericite, and trace-to-rare amounts of ± sericite ± chlorite ± epidote ± zircon ± opaques. A total of 104 thin sections of GQVs have been studied but authigenic zircon grains, glauconite and tourmaline earlier reported by Mishra and Sharma (1975) are not found. Small sericite clots are found enclosed within quartz grains and at places along grain boundaries. The grain size in giant quartz veins is highly variable. Most of these veins are crystalline and fine- to medium-grained, but a few cherty varieties are also found. Breccia texture is abundant with large angular clasts set in a fine-grained quartz matrix. Micro-veins of different generations are present and they are observed to offset one another (figure 4a). Undulatory extinction and deformation lamellae in them are common in quartz (figure 4b). According to Passchier and Trouw (1996), 'sweeping' undulose extinction and deformation lamellae in quartz are the characteristic structures of low-grade conditions (300–400°C). Most quartz grains within micro-veins show polygonization with some showing serrated margins. Sutured and serrated grain boundaries are evidences of bulging recrystallisation (Stipp *et al* 2002). Earlier bands of quartz are transected by bands of new grains formed by dynamic recrystallization. Some of the quartz grains show growth zoning (figures 4c, d), which may reflect trace element compositional changes across the grain profile and/or abundance of submicron sized inclusions. The wide variability in mesoscopic properties of quartz discussed earlier, and the zoning in quartz observed under microscope suggest that quartz precipitated from a polygenic silica-rich hydrothermal fluid. It is notable that in the case of hydrothermal quartz, compositional zoning is more dominant than the self-organized oscillatory zoning, resorption surfaces are absent and cross-cutting of growth zones is not observed (Müller 2000).

5. Geochemistry of giant quartz veins and its implications

Chemical analyses of 26 quartz vein bulk samples are given in table 1. Twenty three samples are from the GQVs, and three samples are

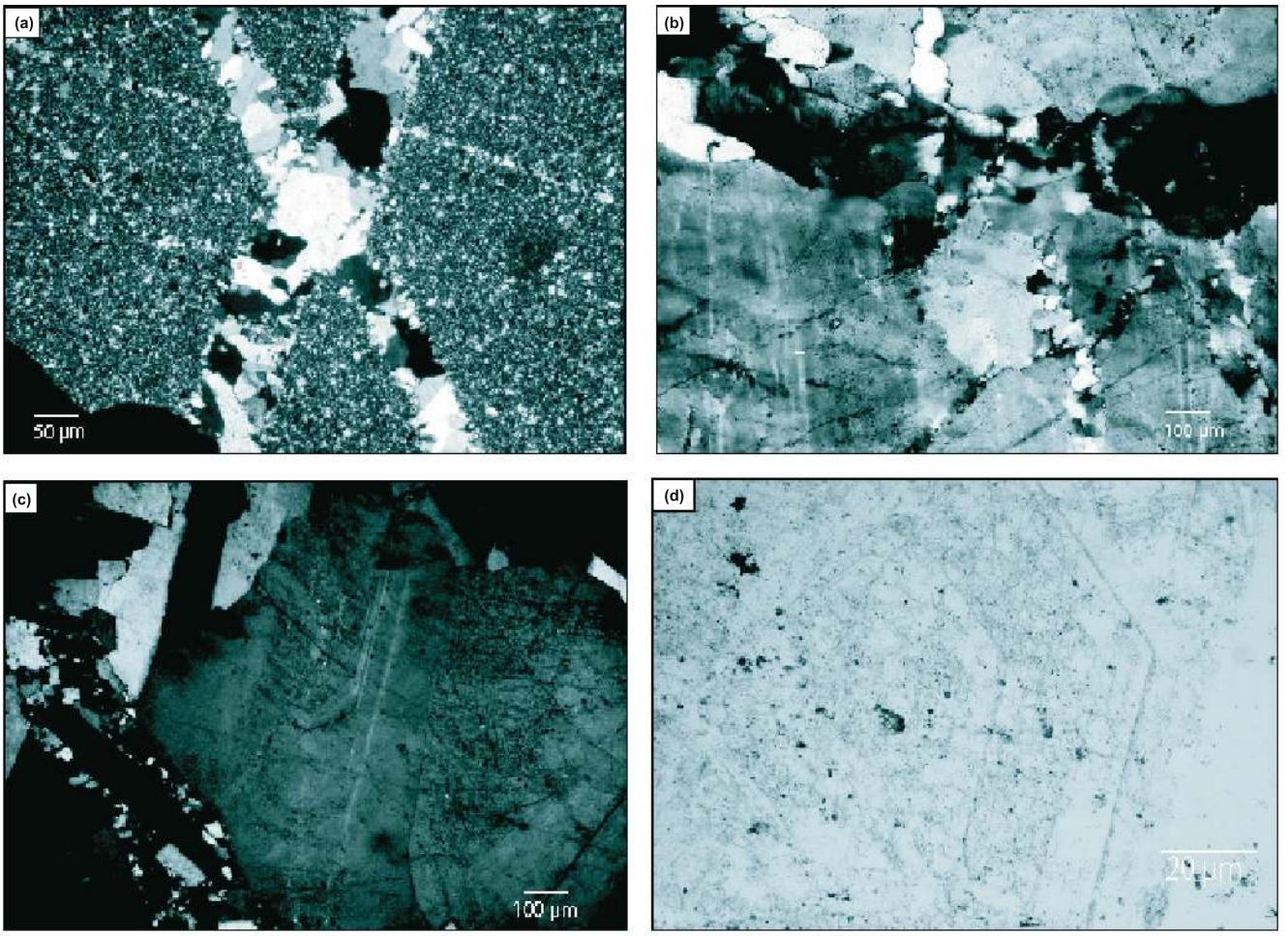

Figure 4. Photomicrographs under crossed nicols. **(a)** Thin cross-cutting veins of crystalline quartz within a sample of giant quartz vein of fine-grained ('cherty') variety. **(b)** Giant quartz vein sample showing undulose extinction and well-developed deformation lamellae suggesting crystal plastic deformation of quartz. **(c)** Zoned quartz grain (centre) with zones of variable thickness which is cut across by a late quartz vein (left). **(d)** Close-up photomicrograph of a zoned quartz grain. Zoning may be the result of trace element compositional changes across the grain profile and/or abundance of sub-micron sized inclusions.

from relatively small quartz veins within granitoid. Out of the latter, one sample is medium-grained (BMQS286), and two samples are very coarse-grained (BMQS281, BMQS290). The samples were broken into small chips and hand picked to avoid any surficial contamination or impurities. The quartz vein chips (± matrix) were translucent-to-opaque and were of varied colours as mentioned in table 1. Samples were ground in steps in an electrically-driven agate mortar to −200 mesh. The powdered samples were then processed for chemical analysis. Elemental analyses except REEs were made using an ICP-AES (JY-JOBIN YVON 70 model). For the sample BGM-34, initial values of some elements were obtained by XRF technique. Calibration of ICP-AES was carried out using the standards BRGM-51, 52, and 53 (BRGM, France). The analytical precision is between 5 and 10%. The REEs were analyzed with the help of Instrumental Neutron Activation Analytical method at the Chemical Laboratory, GSI (WR), Pune with a precision of 2 to 5%.

The bulk chemical compositions of the quartz vein samples analysed are variable to a considerable extent. The SiO_2 contents of the samples are between 84 and 96 wt% which indicate the presence of phases other than quartz even after considering the analytical precision of 5–10 wt% and ignoring the volatile content that may not exceed 1 wt%. The main accessory phases are K-feldspar and sericite which together amount to a total of up to 10 volume%. The SiO_2 content of crystalline quartz veins is, in general, high compared to cherty quartz veins. The Al_2O_3 content lies between <1 and 6.4 wt% and exhibits a positive correlation with the K_2O content (figure 5a) indicating the possible presence of potash feldspar and/or sericite. The total iron contents

Table 1. *Chemical analyses of 23 representative samples of giant quartz veins, and 3 samples of small quartz veins in granite from different parts of the Bundelkhand Craton. Oxide values are in wt%, and trace element concentrations are in ppm. REE analyses of one sample each of migmatite leucosome, alkali feldspar granite and granodiorite from the Bundelkhand Craton are given for comparison.*

Sample no	BMQS280	BMQS439	BMQS342	BGM34	BMQS-55	BMQS50	BMQS363	BMQS290
Colour*	M. white	Pink	Green	G. grey	G. grey	G. grey	G. grey	M. white
Texture**	Cr	Cr	Ch	Cr	Cr	Cr	Cr	Cr
Source***	Drusy	GQV	GQV	GQV	GQV	GQV	GQV	GQV
SiO_2	87.7	92.8	94.4	94.19	n.d.	n.d.	n.d.	90.3
TiO_2	0.02	0.04	0.02	0.02	n.d.	n.d.	n.d.	0.02
Al_2O_3	3.1	< 1	1.9	1.29	n.d.	n.d.	n.d.	< 1
Fe_2O_3(T)	0.82	1.8	0.92	1.82	n.d.	n.d.	n.d.	0.68
CaO	< 1	< 1	< 1	0.35	n.d.	n.d.	n.d.	< 1
MgO	< 1	< 1	< 1	0.5	n.d.	n.d.	n.d.	< 1
Na_2O	< 0.5	< 0.5	< 0.5	0.42	n.d.	n.d.	n.d.	< 0.5
K_2O	1.1	< 0.5	< 0.5	0.24	n.d.	n.d.	n.d.	< 0.5
MnO	< 0.01	< 0.01	0.01	0.02	n.d.	n.d.	n.d.	< 0.01
Total	92.74	94.64	97.25	98.85				90.7
P	< 100	3051	< 100	0.02	n.d.	n.d.	n.d.	< 100
Li	< 10	< 10	< 10	< 10	n.d.	n.d.	n.d.	< 10
Be	< 2	< 2	< 2	< 2	n.d.	n.d.	n.d.	< 2
B	< 10	< 10	11	< 10	n.d.	n.d.	n.d.	< 10
V	< 10	< 10	< 10	< 10	n.d.	n.d.	n.d.	< 10
Cr	< 10	< 10	56	6.3	n.d.	n.d.	n.d.	< 10
Co	< 5	< 5	< 5	< 5	n.d.	n.d.	n.d.	< 5
Ni	< 10	< 10	35	< 10	n.d.	n.d.	n.d.	< 10
Cu	631	< 5	37	30	n.d.	n.d.	n.d.	< 5
Zn	94	< 5	20	10	n.d.	n.d.	n.d.	< 5
Pb	107	59	63	155	n.d.	n.d.	n.d.	61
As	< 20	60	21	< 20	n.d.	n.d.	n.d.	29
Sr	80	18	12	10	n.d.	n.d.	n.d.	< 5
Y	< 20	< 20	< 20	< 20	n.d.	n.d.	n.d.	< 20
Nb	< 20	< 20	< 20	< 20	n.d.	n.d.	n.d.	< 20
Mo	6	6	25	20	n.d.	n.d.	n.d.	8
Ag	< 1.0	< 1.0	< 1.0	< 1.0	n.d.	n.d.	n.d.	< 1.0
Cd	< 2	< 2	2	< 2	n.d.	n.d.	n.d.	< 2
Sn	< 20	< 20	27	< 20	n.d.	n.d.	n.d.	< 20
Sb	< 10	< 10	< 10	< 10	n.d.	n.d.	n.d.	< 10
Ba	< 10	15	70	20	n.d.	n.d.	n.d.	< 10
La	2.8	6.6	5.9	3.03	2.4	0.88	1.6	0.82
Ce	6.7	13	12	6.5	5.6	2	2.9	1.9
Nd	4.8	5.8	5.2	1.31	3.9	1.2	1.3	1.2
Sm	1.1	0.8	0.64	0.27	1.3	0.34	0.3	0.34
Eu	0.11	0.29	0.19	0.09	0.46	0.12	0.1	0.12
Tb	0.3	0.17	0.09	0.05	0.29	0.08	0.06	0.07
Yb	2.4	0.52	0.22	0.07	1.3	0.34	0.19	0.27
Lu	0.4	0.08	0.03	0.01	0.19	0.05	0.03	0.04

*B: brick; G: greenish; M: milky; P: purplish.
**Cr: crystalline; Ch: cherty.
***GQV: giant quartz vein; Peg: quartz pegmatite vein; QVIG: quartz vein in granite; PQVIG: very coarse-grained quartz vein in granite; ML: migmatite leucosome; AFG: alkali feldspar granite; GR: granodiorite.
n.d.: not determined.

expressed as Fe_2O_3 for fifteen quartz vein samples are less than 1 wt%, but the maximum is 3.6 wt% and the minimum is as low as 0.34 wt%. The total iron content does not have any correlation with the colour of the samples although the pinkish brown coloured quartz contains the maximum total iron analyzed. The TiO_2 concentrations in the quartz vein samples are between <0.01 and

Table 1. *(Continued)*

Sample no	BMQS11	BMQS249	BMQS264	BMQS279	BMQS286	BMQS359	BMQS391	BMQS454
Colour*	M. white	B. red	P. grey	Grey	M. white	Grey	G. grey	G. grey
Texture**	Cr	Cr	Ch	Cr	Cr	Ch	Cr	Ch
Source***	GQV	GQV	GQV	GQV	QVIG	GQV	GQV	GQV
SiO_2	94.1	83.7	87.6	85.4	86.6	93.3	93.7	92.1
TiO_2	0.01	0.12	0.03	0.01	0.03	0.01	0.03	1.07
Al_2O_3	< 1	3.8	1.6	1.8	6.4	1.5	< 1	3
Fe_2O_3(T)	0.87	1.6	0.71	3.4	0.57	0.78	1.6	0.66
CaO	< 1	< 1	< 1	< 1	< 1	< 1	< 1	< 1
MgO	< 1	< 1	< 1	1.4	< 1	< 1	< 1	< 1
Na_2O	< 0.5	< 0.5	< 0.5	< 0.5	< 0.5	< 0.5	< 0.5	< 0.5
K_2O	< 0.5	0.9	< 0.5	< 0.5	2.3	< 0.5	< 0.5	0.7
MnO	< 0.01	< 0.01	0.01	0.04	0.01	< 0.01	0.01	< 0.01
Total	94.98	90.12	89.95	92.05	95.91	95.59	95.34	97.53
P	< 100	< 100	< 100	< 100	< 100	< 100	< 100	< 100
Li	< 10	< 10	< 10	35	< 10	< 10	< 10	< 10
Be	< 2	< 2	< 2	< 2	< 2	< 2	< 2	< 2
B	< 10	19	< 10	< 10	< 10	< 10	< 10	< 10
V	< 10	< 10	< 10	< 10	< 10	< 10	< 10	< 10
Cr	< 10	< 10	< 10	< 10	< 10	< 10	< 10	< 10
Co	7	< 5	< 5	7	< 5	< 5	35	< 5
Ni	< 10	< 10	< 10	< 10	< 10	< 10	< 10	< 10
Cu	6	< 5	< 5	< 5	18	20	13	5
Zn	< 5	7	< 5	25	18	< 5	5	6
Pb	81	50	54	56	100	54	60	32
As	54	< 20	< 20	77	< 20	< 20	39	< 20
Sr	6	44	10	< 5	18	10	11	11
Y	< 20	< 20	< 20	< 20	< 20	< 20	< 20	< 20
Nb	< 20	< 20	< 20	< 20	< 20	< 20	< 20	< 20
Mo	14	< 5	5	< 5	< 5	35	14	6
Ag	< 1.0	< 1.0	< 1.0	< 1.0	< 1.0	< 1.0	< 1.0	< 1.0
Cd	2	< 2	< 2	< 2	< 2	< 2	< 2	< 2
Sn	< 20	< 20	< 20	< 20	< 20	< 20	< 20	< 20
Sb	< 10	< 10	< 10	< 10	< 10	< 10	< 10	< 10
Ba	< 10	11	116	< 10	74	20	< 10	35
La	0.67	3.7	14	n.d.	n.d.	n.d.	n.d.	n.d.
Ce	1.7	9.6	18	n.d.	n.d.	n.d.	n.d.	n.d.
Nd	1.2	7.2	7.4	n.d.	n.d.	n.d.	n.d.	n.d.
Sm	0.38	2.3	1.2	n.d.	n.d.	n.d.	n.d.	n.d.
Eu	0.14	0.87	0.28	n.d.	n.d.	n.d.	n.d.	n.d.
Tb	0.08	0.56	0.12	n.d.	n.d.	n.d.	n.d.	n.d.
Yb	0.37	2.5	0.5	n.d.	n.d.	n.d.	n.d.	n.d.
Lu	0.06	0.38	0.07	n.d.	n.d.	n.d.	n.d.	n.d.

1.07 wt%. However, twenty samples have values of < 0.05 wt% indicating a lower content of Ti, in general.

The bivariate plots (figures 5b, c, d, e and f) involving SiO_2 and other major oxides do not depict any marked correlation with the SiO_2 content, clearly an indication of the non-igneous origin of the giant quartz veins. The CaO and MgO concentrations are less than 1 wt% each. The TiO_2 and MnO values do not vary with respect to the SiO_2 content, and therefore, may not be residing in quartz. In general, the incorporation of trace elements in quartz of hydrothermal origin is dependent on the growth direction and velocity, solution chemistry and P–T condition of its equilibration (Brown and Thomas 1960; Cohen 1960; Siebers and Klapper 1984; Siebers 1986). The total iron content in quartz is known to be temperature

Table 1. *(Continued)*

Sample no	BMQS382	BMQS281	BMQS13	BMQS19	BMQS33	BMQS34	BMQS141	BMQS173
Colour*	P. brown	M. white	Pink	M. white	G. grey	G. grey	Grey	M. white
Texture**	Cr	Cr	Cr	Cr	Cr	Cr	Cr	Ch
Source***	GQV	PQVIZ	GQV	GQV	GQV	GQV	GQV	GQV
SiO_2	90.4	92	95.7	95.5	92.9	94.9	92.4	86.3
TiO_2	0.67	< 0.01	< 0.01	0.01	0.04	0.01	0.01	0.05
Al_2O_3	3.1	< 1	< 1	1	< 1	< 1	< 1	3.2
Fe_2O_3(T)	3.6	0.86	0.34	0.87	2.7	0.76	1.1	0.73
CaO	< 1	< 1	< 1	< 1	< 1	< 1	< 1	< 1
MgO	< 1	< 1	< 1	< 1	< 1	< 1	< 1	< 1
Na_2O	< 0.5	< 0.5	< 0.5	< 0.5	< 0.5	< 0.5	< 0.5	< 0.5
K_2O	< 0.5	< 0.5	< 0.5	< 0.5	< 0.5	< 0.5	< 0.5	0.9
MnO	< 0.01	< 0.01	< 0.01	< 0.01	0.01	0.01	0.01	0.01
Total	97.77	92.86	96.04	97.38	95.65	95.68	93.52	91.19
P	< 100	< 100	< 100	< 100	< 100	< 100	< 100	< 100
Li	< 10	< 10	< 10	< 10	15	< 10	< 10	< 10
Be	< 2	< 2	< 2	< 2	< 2	< 2	< 2	< 2
B	< 10	< 10	< 10	< 10	15	< 10	< 10	< 10
V	< 10	< 10	< 10	< 10	< 10	< 10	< 10	< 10
Cr	< 10	< 10	< 10	< 10	< 10	< 10	< 10	< 10
Co	< 5	< 5	6	7	75	8	12	< 5
Ni	< 10	< 10	< 10	10	11	< 10	< 10	< 10
Cu	< 5	< 5	< 5	< 5	11	6	< 5	< 5
Zn	7	< 5	13	5	11	8	6	13
Pb	564	51	90	75	78	80	52	59
As	75	< 20	48	51	80	67	41	< 20
Sr	10	< 5	6	8	8	11	8	20
Y	23	< 20	< 20	< 20	< 20	< 20	< 20	< 20
Nb	< 20	< 20	< 20	< 20	< 20	< 20	< 20	< 20
Mo	7	8	14	13	30	15	8	52
Ag	< 1.0	< 1.0	< 1.0	< 1.0	< 1.0	< 1.0	< 1.0	< 1.0
Cd	< 2	< 2	2	3	3	3	< 2	< 2
Sn	< 20	< 20	< 20	< 20	21	< 20	< 20	< 20
Sb	< 10	< 10	< 10	< 10	< 10	< 10	< 10	< 10
Ba	20	< 10	< 10	< 10	< 10	< 10	< 10	38
La	n.d.	n.d.	n.d.	n.d.	n.d.	n.d.	n.d.	n.d.
Ce	n.d.	n.d.	n.d.	n.d.	n.d.	n.d.	n.d.	n.d.
Nd	n.d.	n.d.	n.d.	n.d.	n.d.	n.d.	n.d.	n.d.
Sm	n.d.	n.d.	n.d.	n.d.	n.d.	n.d.	n.d.	n.d.
Eu	n.d.	n.d.	n.d.	n.d.	n.d.	n.d.	n.d.	n.d.
Tb	n.d.	n.d.	n.d.	n.d.	n.d.	n.d.	n.d.	n.d.
Yb	n.d.	n.d.	n.d.	n.d.	n.d.	n.d.	n.d.	n.d.
Lu	n.d.	n.d.	n.d.	n.d.	n.d.	n.d.	n.d.	n.d.

dependent and its concentration increases with temperature.

Most of the quartz vein samples containing measurable concentrations of Cu, Zn and Pb when plotted in a triangular diagram (figure 6), cluster near the Pb apex. Figure 7 shows the range of variation of trace elements in the quartz veins with respect to the average upper crust (Taylor and McLennan 1985). The degree of variation is due not only to the dilution effect of quartz, but also to the wide range of mobility of various elements. While Ag, Sb, Cd, Mo, As, Sn and Pb are invariably enriched in the quartz vein samples, Co, Cu, Ni, B, Y, Cr and Zn show enrichment in some and depletion in others. One green-coloured quartz vein sample shows an anomalous content of Cr (56 ppm) which may be due to the presence of accessory fuchsite. Ba and Sr both are greatly depleted. The Sr content varies between 6 and 80 ppm with a mean value of 14 ppm and is significantly less than the upper crustal

Table 1. *(Continued)*

Sample no	BMQS177	BMQS271	BIGS-16C	BGM-16	BGM8
Colour*	Grey	P. brown	–	–	–
Texture**	Ch	Cr	–	–	–
Source***	GQV	GQV	ML	AFG	GR
SiO_2	87.3	89.5	76.9	75.6	69.8
TiO_2	0.03	0.01	n.d.	n.d.	n.d.
Al_2O_3	2.2	< 1	n.d.	n.d.	n.d.
Fe_2O_3(T)	0.63	0.74	n.d.	n.d.	n.d.
CaO	< 1	< 1	n.d.	n.d.	n.d.
MgO	< 1	< 1	n.d.	n.d.	n.d.
Na_2O	< 0.5	< 0.5	n.d.	n.d.	n.d.
K_2O	0.6	< 0.5	n.d.	n.d.	n.d.
MnO	0.01	< 0.01	n.d.	n.d.	n.d.
Total	90.77	90.25			
P	< 100	< 100	n.d.	n.d.	n.d.
Li	< 10	< 10	n.d.	n.d.	n.d.
Be	< 2	< 2	n.d.	n.d.	n.d.
B	< 10	< 10	n.d.	n.d.	n.d.
V	< 10	< 10	n.d.	n.d.	n.d.
Cr	< 10	< 10	n.d.	n.d.	n.d.
Co	< 5	< 5	n.d.	n.d.	n.d.
Ni	< 10	< 10	n.d.	n.d.	n.d.
Cu	18	< 5	n.d.	n.d.	n.d.
Zn	17	< 5	n.d.	n.d.	n.d.
Pb	66	54			
As	< 20	33	n.d.	n.d.	n.d.
Sr	20	6	n.d.	n.d.	n.d.
Y	20	< 20	n.d.	n.d.	n.d.
Nb	< 20	< 20	n.d.	n.d.	n.d.
Mo	< 5	7	n.d.	n.d.	n.d.
Ag	< 1.0	< 1.0	n.d.	n.d.	n.d.
Cd	< 2	< 2	n.d.	n.d.	n.d.
Sn	< 20	< 20	n.d.	n.d.	n.d.
Sb	< 10	< 10	n.d.	n.d.	n.d.
Ba	191	< 10	n.d.	n.d.	n.d.
La	n.d.	n.d.	15.15	27	92.9
Ce	n.d.	n.d.	23.37	64	114.83
Nd	n.d.	n.d.	9.09	22	38.39
Sm	n.d.	n.d.	1.81	4.1	3.52
Eu	n.d.	n.d.	0.6	0.52	1.01
Tb	n.d.	n.d.	0.22	0.64	0.5
Yb	n.d.	n.d.	0.47	1.1	0.99
Lu	n.d.	n.d.	0.06	0.12	0.13

average of 350 ppm. This mean value is even lower than most sedimentary rocks, but is much higher than in quartz reported from metamorphic and some hydrothermal environments (Monecke *et al* 2002). Such unusually high Sr content in the quartz veins can be attributed to Sr release during feldspar alteration in the wall rocks by hydrothermal fluid. Be, Nb and V apparently are less variable because of their concentration falling below the resolution of the instrument. Pati *et al* (1997) reported that some of the quartz veins are auriferous (up to 0.25 ppm Au). The obvious enrichment of the chalcophile elements Ag, Sb, Cd, Mo, As, Sn and Pb along with the presence of sulfide minerals in the quartz veins at places clearly indicates a hydrothermal process responsible for their transport and precipitation. Chalcopyrite and malachite which are locally associated with quartz veins occurring within granitoids exhibit comb structure, suggesting precipitation from a fluid (Dong *et al* 1995).

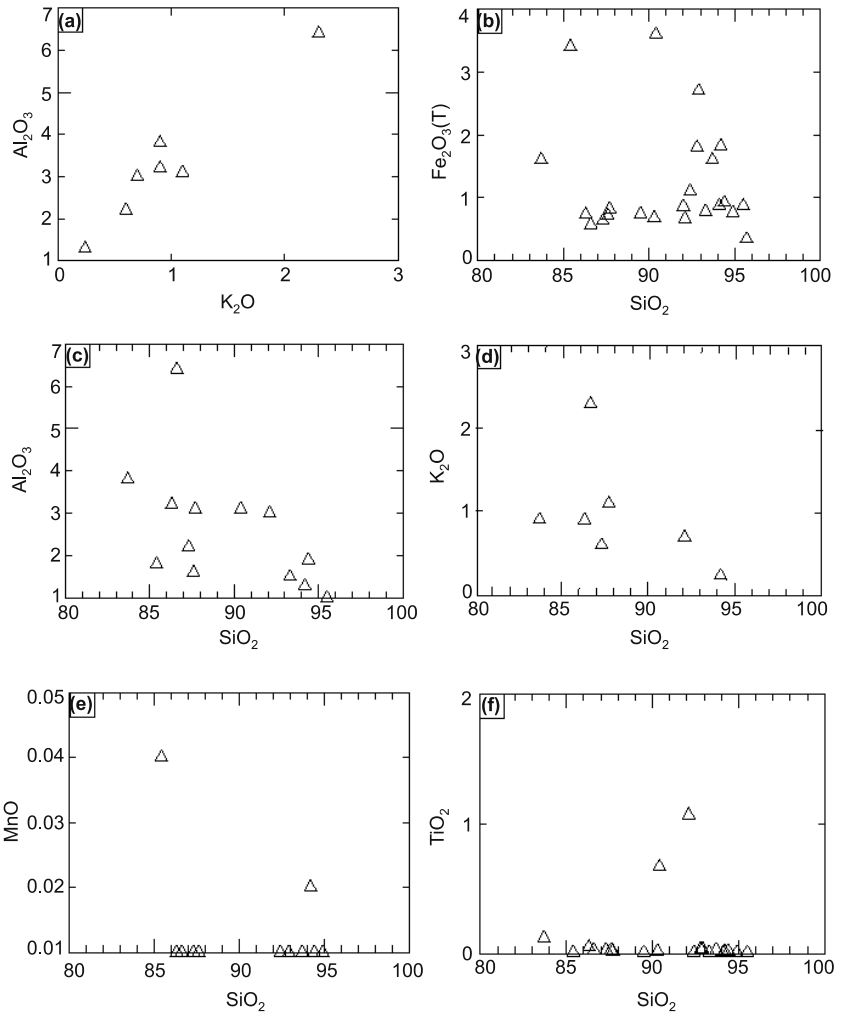

Figure 5. Bivariant major oxide plots (a–f) of GQVs. Only those samples with appreciable content of different oxides have been plotted. Positive correlation is seen between Al_2O_3 and K_2O (5a). SiO_2 *versus* major oxides (5b–5f) depict a scatter for elements such as Fe_2O_3 (T), Al_2O_3, K_2O, MnO and TiO_2, respectively.

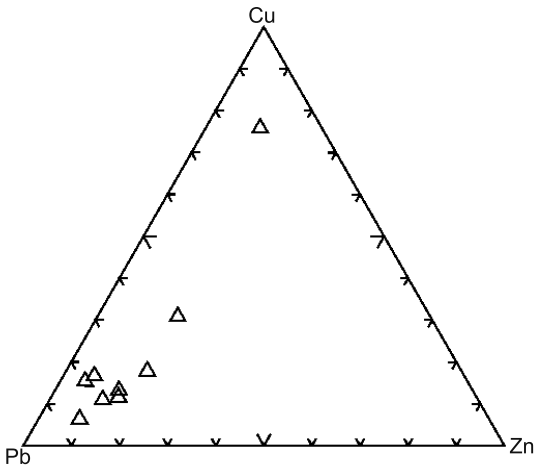

Figure 6. Composition of GQVs in the triangular plot of Cu, Pb and Zn.

Chondrite normalized rare earth elements (REE) patterns of ten samples of GQVs and one sample (BMQS290) of a relatively small, very coarse-grained quartz vein within granite are compared with those of hydrothermal quartz of Monecke *et al* (2002), and alkali feldspar granite (BGM-16), granodiorite (BGM-8), and migmatite leucosome (BIGS-16C) from the Bundelkhand Craton (figures 8a, b, c). The REE concentrations in the giant quartz veins are variable but very high compared to the vein quartz of Monecke *et al* (2002). This is attributed to the presence of K-feldspar in the quartz veins. Elevated concentrations of REE in the migmatite leucosome and alkali feldspar granite (figure 8c) corroborate this inference because K-feldspar is the main host of REE in these rocks. In the quartz veins the REE concentration is found to be inversely proportional to the SiO_2 content which suggests that decrease in REE abundance is because of dilution by increasing amounts of quartz.

Monecke *et al* (2002) compared the REE patterns of hydrothermal vein quartz and

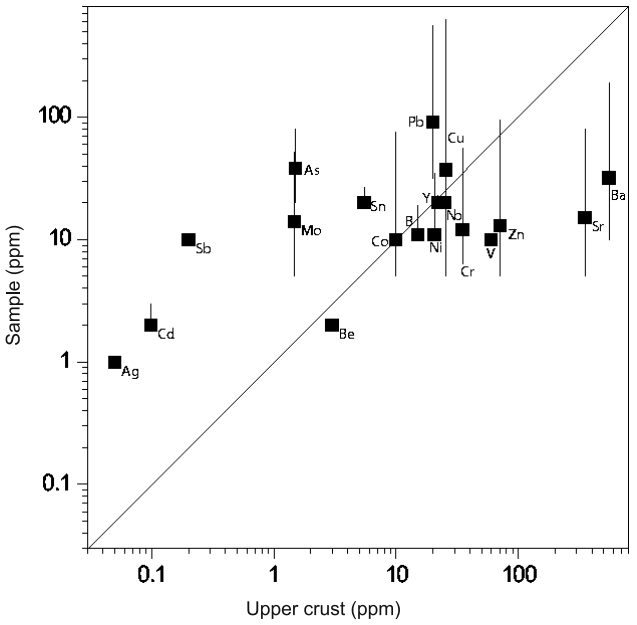

Figure 7. Trace element concentrations of quartz vein samples plotted against their upper crustal abundances (Taylor and McLennan 1985). Bars span the range of concentrations and filled squares represent average concentration for each element.

metamorphic quartz. They observed, in the case of metamorphic quartz, LREE*n* enriched and HREE*n* depleted lanthanide distribution patterns with variable positive Ce anomalies. On the other hand, hydrothermal vein quartz shows variable enrichments of HREE*n* and common positive Eu anomalies. In some cases, hydrothermal vein quartz has flat HREE*n* patterns. Four samples of GQVs and the sample BMQS290 from the small quartz vein within granite from the Bundelkhand Craton show nearly flat HREE*n* and negligible or slight LREE*n* enrichment, and are comparable, except for the lack of positive Eu anomaly, to two samples (KS-4 and KS-5) of hydrothermal vein quartz of Monecke *et al* (2002) (figure 8a). Four samples of quartz veins (BMQS264, BMQS342, BMQS363 and BMQS439) show nearly smooth, LREE*n* enriched, and either HREE*n* depleted or flat patterns, which bear considerable similarity to that of another sample (L-13) of hydrothermal vein quartz of Monecke *et al* (2002) (figure 8b).

Two samples (BGM34 and BMQS280) of GQVs show unique REE patterns (figure 8c). Sample BGM34 shows a step-wise decrease from LREE*n* to HREE*n*, whereas sample BMQS280 shows a flat LRRE*n*, negative Eu anomaly, *albeit* semi-quantitative, and highly enriched HREE*n* pattern. This unusual HREE*n* enrichment could be due to the possible presence of trace amounts of zircon in the sample. However, the above similarities in the REE patterns of the GQVs of the Bundelkhand Craton and the hydrothermal quartz of Monecke *et al* (2002) lend support to a hydrothermal origin of the former despite the fact that their REE signatures are controlled mainly by K-feldspar.

6. Discussion

Roday *et al* (1995) have noted, "... quartz reefs are genetically related to the development of ductile shear zones within the granitic rocks and brittle–ductile shears in the intervening wall rocks". They also suggested that these quartz veins are basically co-genetic melt secreted product of microgranites. Our geochemical data, however, do not favour a magmatic origin of these veins. Furthermore, in terms of volume, the giant quartz veins would require high fluid pressure (P_{fluid}) to drive the granitic minimum to the quartz-rich end, if the igneous origin is to be accepted. The high P_{fluid}, if existed, would have resulted in the formation of large volumes of granitic pegmatites. However, unlike the Singhbhum and other granitoid complexes of India, the Bundelkhand Granitoid Complex is conspicuously devoid of granitic pegmatites ruling out the magmatic origin hypothesis of the quartz veins.

The lack of earlier reported so-called sedimentary structures, and heavy minerals such as authigenic zircon, glauconite, tourmaline and mica (Mishra and Sharma 1975) discourages us to propose a sedimentary origin for the GQVs. On the other hand, Sharma and Rahman (1996) have mentioned that these giant quartz veins represent "the late stage singular hydrothermal process in the evolution of the Bundelkhand batholith". Our geochemical findings support the idea of Sharma and Rahman (1996) pertaining to the hydrothermal origin but advocate polyphase fluid activity. Field, petrographic and geochemical data suggest that precipitation of silica from hydrothermal fluids in tectonically-controlled weak planes is the most plausible mechanism for the origin of GQVs of the Bundelkhand craton. However, source(s) of such hydrothermal fluids cannot be unambiguously established.

Acknowledgements

JKP thanks Mr. Ravi Shankar, Director General (Retd.), GSI, since a part of this work was carried out under his constant support and encouragement when he was the Dy Director General, GSI, NR (Lucknow). Mr. V D Mamgain, Dy Director General (Retd.), GSI, Op. U.P., is heartily thanked

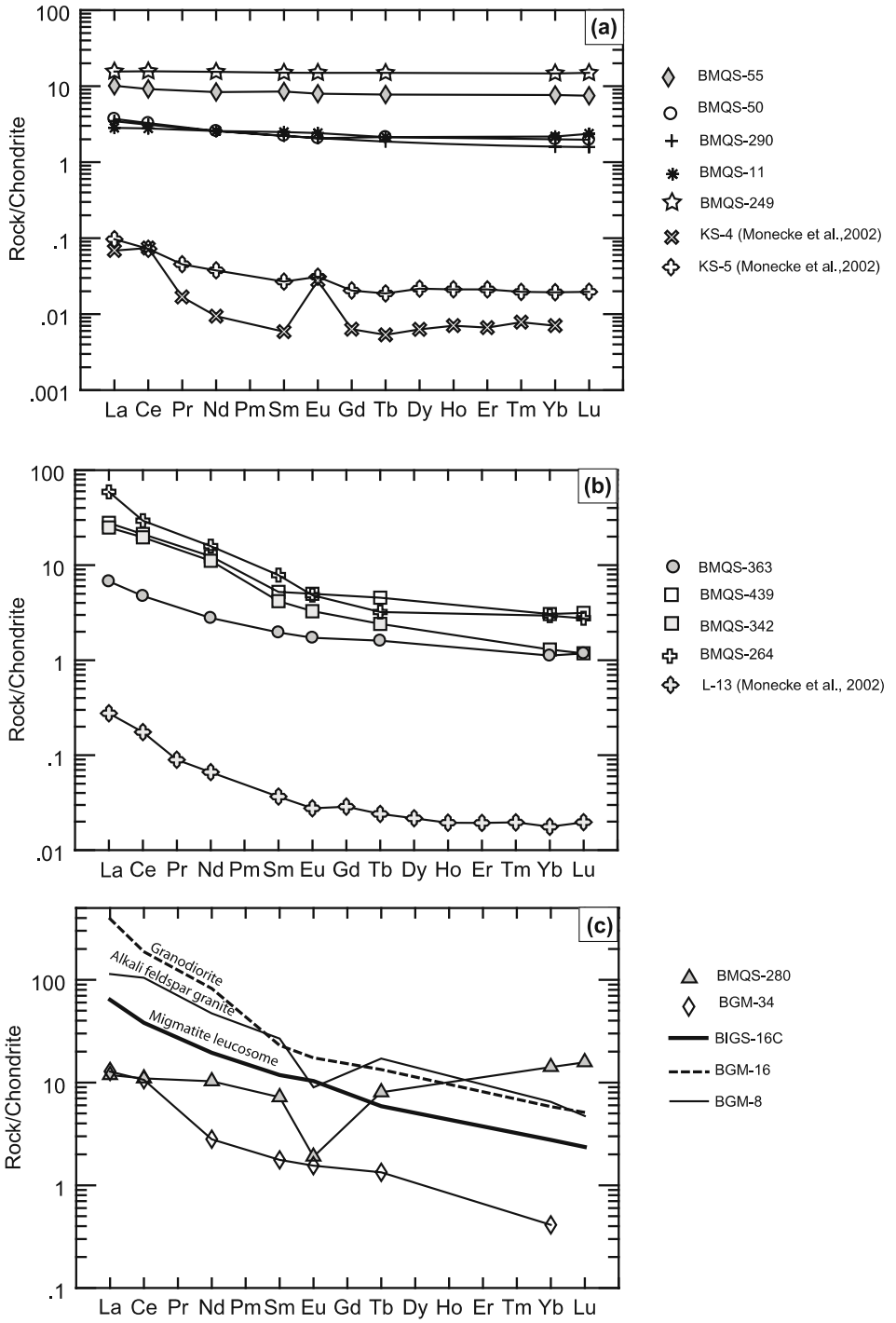

Figure 8. Chondrite normalised (Sun and McDonough 1989) REE patterns of quartz veins. **(a)** Nearly flat pattern in four samples of GQVs and one sample (BMQS290) of a small quartz vein within granite. Two samples of hydrothermal quartz of Monecke *et al* (2002) are shown for reference. **(b)** Plot of four samples of GQVs showing LREEn enriched and HREEn depleted or flat pattern. A third sample of hydrothermal quartz of Monecke *et al* (2002) is shown for reference. **(c)** Patterns of two samples of GQVs, and one sample each from migmatite leucosome (BIGS-16C), alkali feldspar granite (BGM-16), and granodiorite (BGM-8) from the Bundelkhand Craton.

for his great insight, help and tremendous encouragement during his tenure as the Director, STM-P, Op. U.P. (Lucknow). Dr. Thomas Monecke, Institute for Mineralogy, Technical University of Bergakademie, Freiberg, Germany is sincerely thanked for kindly sending all the required reprints and other necessary data. We thank Dr. Wanming Yuan, Dr. Tom Andersen, and Dr. Biswajit Mishra for their thorough, critical and constructive reviews.

References

Basu A K 1986 Geology of parts of the Bundelkhand Craton, central India; *Rec. Geol. Surv. India* **101** 61–124.

Brown C and Thomas L 1960 The effect of impurities on the growth of synthetic quartz; *J. Phys. Chem. Solids* **13** 337.

Cohen A 1960 Substitutional and interstitial aluminium impurity in quartz: structure, and colour centre interrelationships; *J. Phys. Chem. Solids* **13** 321–325.

Dong G, Morrison G and Jaireth S 1995 Quartz textures in epithermal veins, Queensland – classification, origin and implication; *Econ. Geol.* **90** 1841–1856.

Gaines RV, Skinner H C W, Foord E E, Mason B and Rosenzweig A 1997 *Dana's New Mineralogy* (New York: John Wiley & Sons) 1819 p.

Jhingran A G 1958 The problem of Bundelhkand granites and gneisses. Presidential Address; *Proc. 45th Indian Sci. Cong.*, Madras 98–120.

Kerrich R and Feng R 1992 Archean geodynamics and the Abitibi-Pontiac collision: implications for advection of fluids at transpressive collisional boundaries and the origin of giant quartz vein systems; *Earth Sci. Rev.* **23** 33–60.

Malviya V P, Arima M, Pati J K and Kaneko Y 2004 First report of metamorphosed pillow lava in central part of Bundelkhand craton – an island arc setting of possible late Archaean age; *Gondwana Res.* **7** 1338–1340.

Malviya V P, Arima M, Pati J K and Kaneko Y 2006 Petrology and geochemistry of metamorphosed basaltic pillow lava and basaltic komatiite in the Mauranipur area: subduction related volcanism in the Archaean Bundelkhand craton, central India; *J. Mineral. Petrol. Sci.* **101** 199–217.

Mishra R C 1960 Quartz reefs of Bundelkhand and their origin; *Proc. Indian Sci. Cong.*, **III** 241–242.

Mishra R C and Sharma R P 1975 New data on the geology the Bundelkhand Complex of central India; *Recent Researches in Geology* (New Delhi: Hindustan Publishing Corporation) 311–346.

Mondal M E A, Goswami J N, Deomurari M P and Sharma K K 2002 Ion microprobe 207Pb/206Pb ages zircons from Bundelkhand craton, north India: implications for crustal evolution of the Bundelkhand–Aravalli protocontinent; *Prec. Res.* **117** 85–100.

Monecke T, Kempe U and Götze J 2002 Genetic significance of the trace element content in metamorphic and hydrothermal quartz: a reconnaissance study; *Earth Planet. Sci. Lett.* **202** 709–724.

Müller A 2000 *Cathodoluminescence and characterisation of defect structures in quartz with applications to the study of granitic rocks* (A dissertation zur Erlangung des Doktorgrades der Mathematisch-Naturwissenschaftlichen Fakultäten der Georg August-Universität zu Götingen) 219 p.

Pascoe E H 1950 *A Manual of the Geology of India and Burma. Part I (3rd edn.)* (Geol. Surv. India) 486 p.

Passchier C W and Trouw R A J 1996 *Microtectonics* (Berlin: Springer-Verlag) 289 p.

Pati J K 1998 Specialized thematic studies of quartz reefs and mylonite zones in parts of Bundelkhand Granitoid Complex, southern U.P.; *Rec. Geol. Surv. India* **130(8)** 88–89.

Pati J K 1999 Study of granitoid mylonites and reef/vein quartz in parts of Bundelkhand Granitoid Complex (BGC); *Rec. Geol. Surv. India* **131(8)** 95–96.

Pati J K, Raju S, Mamgain V D and Shankar R 1997 Record of gold mineralization in parts of Bundelkhand Granitoid Complex (BGC); *J. Geol. Soc. India* **50** 601–606.

Prasad M H, Hakim A and Krishna Rao B 1999 Metavolcanic and metasedimentary inclusions in the Bundelkhand Granitic Complex in Tikamgarh district, Madhya Pradesh; *J. Geol. Soc. India* **54** 359–368.

Rao M J, Poornachandra Rao G V S, Widdowson M and Kelley S P 2005 Evolution of Proterozoic mafic dyke swarms of the Bundelkhand Granite Massif, central India; *Curr. Sci.* **88** 502–506.

Roday P P, Diwan P and Singh S 1995 A synkinematic model of emplacement of quartz reefs and subsequent deformation patterns in the central Indian Bundelkhand batholith; *Proc. Indian Acad. Sci. (Earth Planet. Sci.)* **104** 465–468.

Sarkar A, Bhalla J K, Bishui P K, Gupta S N, Singhai R K and Upadhaya T P 1994 Tectonic discrimination of granitic rocks: studies on the early Proterozoic Bundelkhand Complex, central India; *Indian Minerals* **45** 103–112.

Saxena M N 1961 Bundelkhand granites and associated rocks from Kabrai and Mauranipur area of Hamirpur and Jhansi District, Uttar Pradesh. *Res. Bull (N.S). Punjab Univ.* **12(1-2)** 85–107.

Senthiappan M 1976 Geology of the area along the Raksa Shear zone, Jhansi district, Uttar Pradesh; Symposium on the Archaean of central India, GSI, Nagpur, Nov. 30–Dec. 1 (Abstract), 22 p.

Senthiappan M 1981 Geology of the area along the Raksa Shear zone, Jhansi district, Uttar Pradesh; *Spec. Publ. Geol. Surv. India* **3** 73–76.

Sharma R P 1979 Origin of the pyrophyllite-diaspore deposits of the Bundelkhand Complex, central India; *Mineral Deposita* **14** 343–352.

Sharma R P 1982 Lithostratigraphy, structure and petrology of the Bundelkhand Group; In: *Geology of Vindhyachal* (eds) K S Valdiya, S B Bhatia and V K Gaur (New Delhi: Hindustan Publishing Corporation) 30–46.

Sharma K K and Rahman A 1996 Bundelkhand Craton, Northern Indian Shield geochemistry, petrogenesis and tectonomagmatic environments; *DST Newsletter* **6** 12–17.

Siebers F B 1986 *Inhomogene verteilung von verunreinigungen in gezüchteten und natürlichen quarzen als funktion der Wachstumsbedingungen und ihr Einfluauf kristallphysikalische eigenschaften* (Thesis, Ruhr-Universität Bochum, Germany) 133 p.

Siebers F B and Klapper H 1984 Zelluläres wachstum und verunreinigungsverteilung im zuchtquarz, aufgezeigt mit röntgentopographie; *Zeitschrift für Kristallographie* **167** 177–178.

Stipp M, Stunitz H, Heilbronner R and Schmid S M 2002 The eastern Tonale fault zone: a 'natural laboratory' for crystal plastic deformation of quartz over a temperature range from 250 to 700°C; *J. Struct. Geol.* **24** 1861–1884.

Sun Ss- and McDonough W F 1989 Chemical and isotopic systematics of oceanic basalts implications for mantle composition and process. In: *Magmatism in Ocean Basins* (eds) A D Saunders and M J Norry; Geological Society Special Publication (Netherlands: Kluwer Academic).

Taylor S R and McLennan S M 1985 *The Continental Crust: Its Composition and Evolution* (Oxford: Blackwell Scientific) 311 p.

MS received 31 January 2007; revised 9 May 2007; accepted 25 June 2007